

# Notch Sensitivity of Polycarbonate and Toughened Polycarbonate

Kilwon Cho, JaeHo Yang, Byung Il Kang, Chan Eon Park

Department of Chemical Engineering and Polymer Research Institute, Division of Electrical and Computer Engineering, Pohang University of Science and Technology, Pohang 790-784, Korea

Received 28 October 2002; accepted 3 December 2002

**ABSTRACT:** Notch sensitivity, the effect of a notch radius on the impact behavior of polycarbonate and rubber-toughened polycarbonate, is investigated by using a model based on the slip-lines field theory. Impact strength, determined by the Charpy impact test, was found to increase drastically with an increasing notch radius for pure polycarbonate, whereas the increase of impact strength with increased notch radius was not as extreme for rubber-toughened polycarbonate. These results indicate that the inclusion of rubber particles reduces notch sensitivity. An examination of fracture surfaces reveals that cracks were initiated by internal crazing at some distance from the notch tip for specimens with blunt notches. For pure polycarbonate, the impact

strength is found to have a linear relationship with the square of the notch radius, which is in good agreement with that predicted by the proposed model. However, for rubber-toughened polycarbonate, the linear relationship broke down as the notch radius increased due to the enhanced toughening effect. The proposed model can be applied to clearly explain the notch sensitivity of ductile polymers which exhibit large plastic yielding around the notch tip. © 2003 Wiley Periodicals, Inc. *J Appl Polym Sci* 89: 3115–3121, 2003

**Key words:** notch sensitivity; polycarbonate; toughening; impact strength

## INTRODUCTION

It is well known that the impact behavior of polymers exhibits notch sensitivity, and this behavior has been the subject of intense research.<sup>1–5</sup> A model based on linear elastic fracture mechanics had been proposed by Kinloch and Williams to explain the notch sensitivity of thermosetting polymers.<sup>1</sup> Their model is in good agreement with the experimental observation of brittle polymers. However, their model has not been applied to ductile polymers because it does not consider the large plastic yielding around the notch tip. Vincent suggested the concept of an elastic stress concentration factor in an attempt to rationalize the effect of a notch radius,<sup>2</sup> and this concept has been examined in more detail by Fraser and Ward.<sup>3,4</sup> This model shows good agreement with the experimental observation of polymers exhibiting linear elastic behavior. However, this approach was less successful for ductile polymers such as polycarbonate (PC). Therefore, a model that considers plastic yielding around the notch tip is necessary in order to rationalize the effect of the notch tip radius on the impact behavior of ductile polymers.

In this article, we propose a simple model, namely, the relationship between impact strength and a notch

radius, based on the slip-line field theory<sup>6–9</sup> to rationalize the notch sensitivity of ductile polymers exhibiting large plastic yielding around the notch tip. Verification of the proposed model is reported by using polycarbonate and rubber-toughened polycarbonate.

## MODEL FOR NOTCH SENSITIVITY

In this section we propose a simple relationship between impact strength and notch radius for ductile polymers. For ductile polymers with a blunt notch, plastic deformation occurs around the notch tip on loading. Therefore, the linear elastic fracture mechanics approach is no longer suitable to explain the notch sensitivity of ductile polymers. The stress field inside the plastic deformation region ahead of the notch tip can be described by the slip-lines field theory,<sup>6–9</sup> in which the material is assumed to be pressure independent, perfect plastic.

Based on the slip-lines field theory, for a specimen having a semicircular notch, the principal stresses ahead of the notch tip along the  $x$  axis are given by

$$\sigma_1 = \frac{2}{\sqrt{3}}\sigma_T \left[ 1 + 1n\left(\frac{r}{\rho}\right) \right] \quad (1)$$

$$\sigma_2 = \frac{2}{\sqrt{3}}\sigma_T 1n\left(\frac{r}{\rho}\right) \quad (2)$$

and for the fully plane strain condition,

Correspondence to: K. Cho (kwcho@postech.ac.kr).

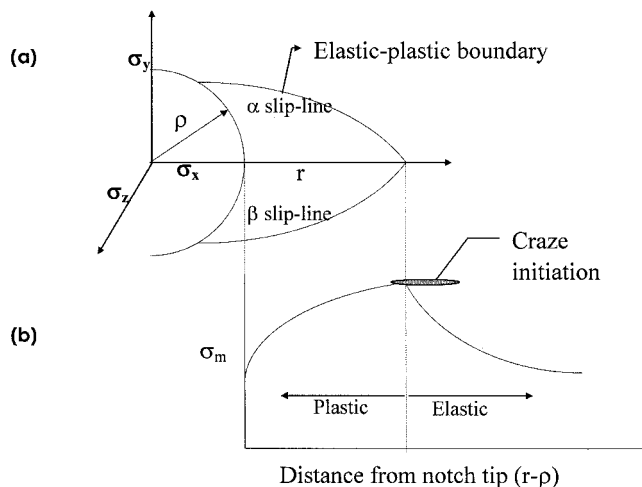


**Figure 1** Schematic diagrams illustrating (a) two slip lines and (b) the mean stress field around the notch tip for the specimen having a notch radius  $\rho$ .<sup>6,7</sup>

$$\sigma_3 = \frac{(\sigma_1 + \sigma_2)}{2} = \frac{2}{\sqrt{3}}\sigma_T \left[ \frac{1}{2} + 1n\left(\frac{r}{\rho}\right) \right] \quad (3)$$

$$\sigma_m = \frac{(\sigma_1 + \sigma_2 + \sigma_3)}{3} = \sigma_3 = \frac{2}{\sqrt{3}}\sigma_T \left[ \frac{1}{2} + 1n\left(\frac{r}{\rho}\right) \right], \quad (4)$$

where  $\omega_m$  is the mean stress,  $\omega_T$  is the tensile yield stress,  $\rho$  is the notch radius, and  $r$  is the distance from the origin according to the  $x$  axis.

The two slip lines for the specimen with a notch radius  $\rho$  are illustrated by the schematic drawing in Figure 1(a). The slip line is the elastic-plastic boundary, that is, the plastically deformed region inside the slip lines is and the elastic region outside the slip lines. The mean stress around the notch tip is shown by the schematic drawing in Figure 1(b). The stress field described by the slip-lines field theory can be applied only in the plastic region. The highest stress occurs at the boundary of the elastic-plastic region. The stress at the boundary of the elastic-plastic region can be obtained by the same stress field as the stress of plastic region, because the stress field is continuous over the elastic-plastic region.

The stress by the slip-lines field theory is independent of the remote stress, as can be seen in eq. (4). As the remote stress increases, the mean stress at the elastic-plastic boundary increases. The increase of remote stress induces the larger plastic deformation, that is, the plastic deformation zone grows outward. When the mean stress,  $\omega_m$ , at the elastic-plastic boundary reaches a critical value for craze initiation  $\omega_{m,cr}$ , the craze failure or so-called internal crazing occurs at the elastic-plastic boundary. The critical mean stress for the nucleation of internal crazes is given by

$$\sigma_m = \sigma_{m,cr} = \frac{2}{\sqrt{3}}\sigma_T \left[ \frac{1}{2} + 1n\left(\frac{r}{\rho}\right) \right] \quad (5)$$

Since the inner side of the slip lines is the plastic region, the length of plastic region  $r_p$  along the  $x$  axis is obtained from eq. (5) as follows:

$$r_p = \exp \left[ \frac{\sqrt{3}\sigma_{m,cr}}{2\sigma_T} - \frac{1}{2} \right] \rho \quad (6)$$

The above equation suggests that plotting the length of the plastic region  $r_p$  as a function of notch radius  $\rho$  should yield a straight line:

$$r_p \sim \rho \quad (7)$$

The total absorbed energy during deformation  $U_t$  is composed of two parts, namely, energy absorption by plastic deformation such as shear yielding,  $U_s$ , and crazing,  $U_c$ . Because the craze fracture is a very brittle fracture, the energy absorbed by crazing is very small compared to the energy absorbed by shear yielding, and  $U_c$  can be ignored. Therefore, the total absorbed energy during deformation by an impact test can be expressed by

$$\begin{aligned} U_t &= U_s + U_c \\ &\cong U_s \end{aligned} \quad (8)$$

The energy absorbed by shear deformation  $U_s$  can be given by

$$U_s = \omega_p \alpha r_p^2 B \quad (9)$$

where  $\omega_p$  is the strain energy density,  $B$  is the specimen thickness, and  $\alpha$  is the shape factor of the deformation zone, that is, when the shape of plastic deformation zone is circular,  $\alpha$  is  $2\pi$ , and for square shape,  $\alpha$  is 1, and so forth. Since  $r_p$  has a linear relation with  $\rho$ ,  $U_s$  is proportional to  $\rho^2$ . Therefore, the total energy absorbed during deformation is linearly related to the square of the notch radius:

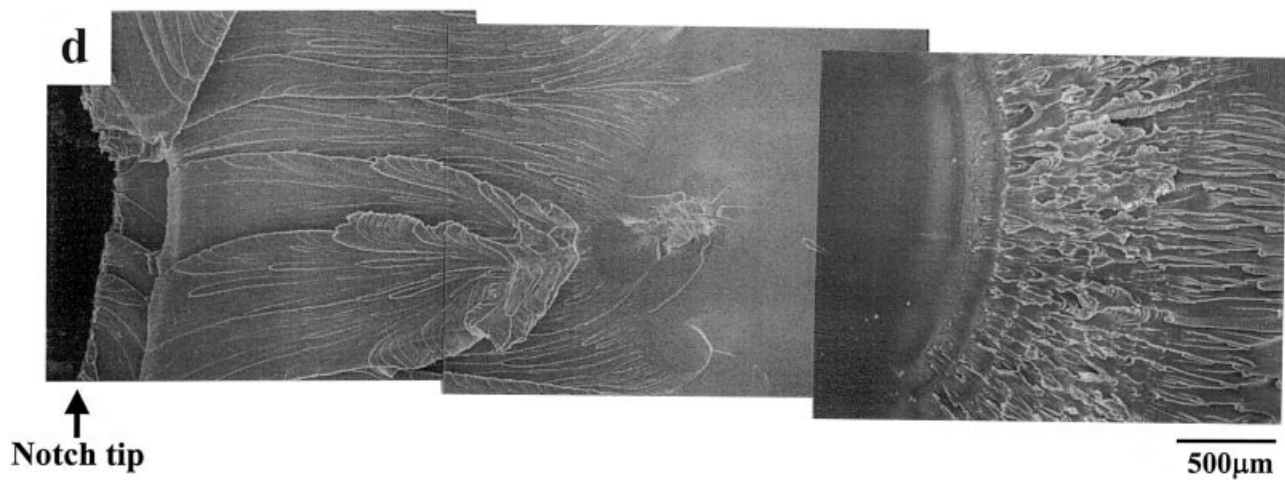
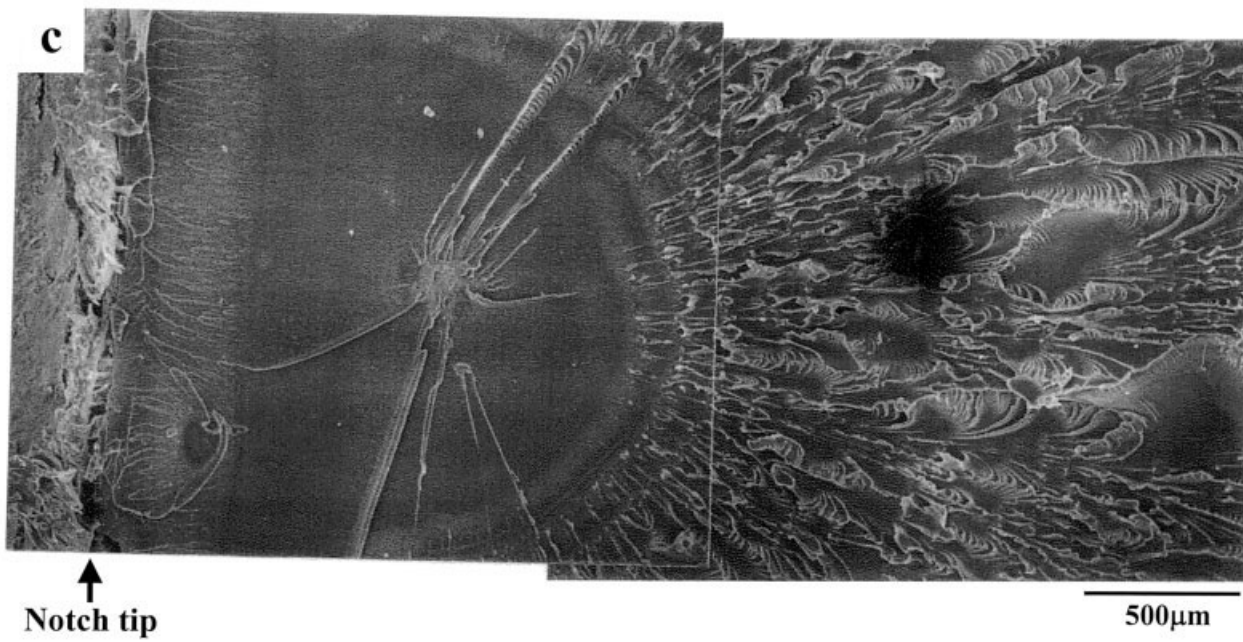
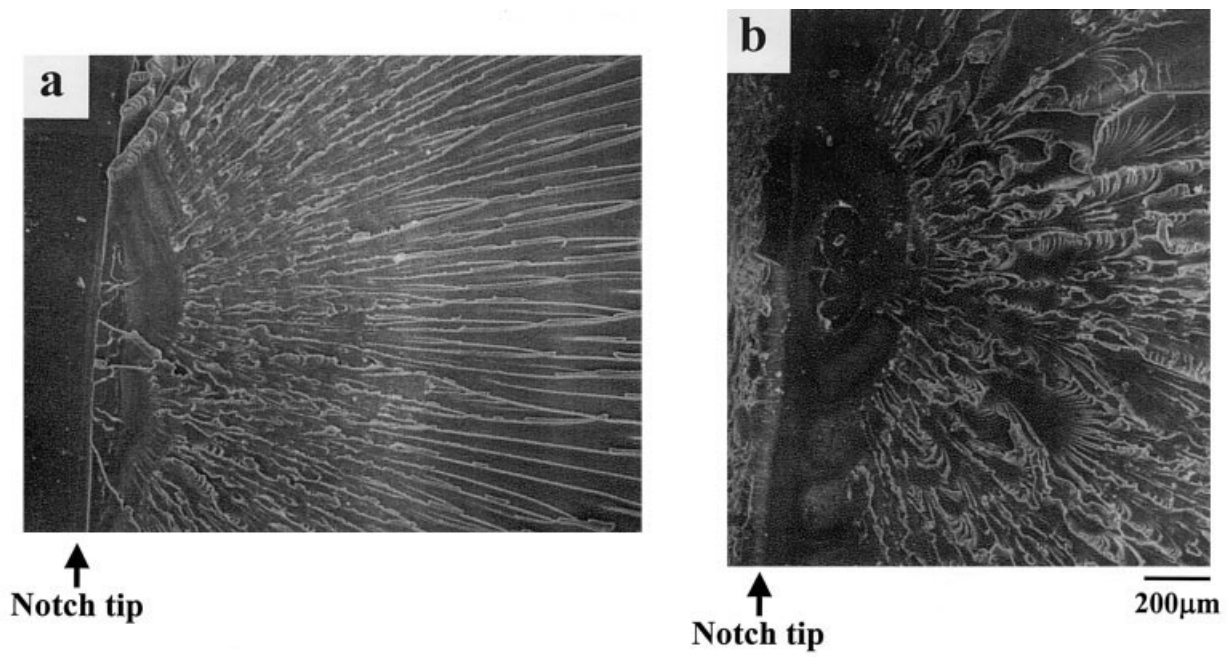
$$U_t \sim \rho^2 \quad (10)$$

## EXPERIMENTAL

### Materials

The matrix material was a bisphenol-A type polycarbonate (PC) (Lexan 141b) obtained from General Elec-

**Figure 2** SEM micrographs of the fracture surface of neat PC. Notch radius: (a) sharp notch, (b) 0.25 mm, (c) 3.37 mm, and (d) 6.15 mm.



tric Co. (Pleasanton, CA). A core-shell type particle was used as an impact modifier, which consists of a rubbery core composed of slightly crosslinked poly(*n*-butyl acrylate) and a glassy shell composed of poly(methyl methacrylate). The average diameter of the rubbery core was 0.32  $\mu\text{m}$ . The rubbery core was slightly cross-linked by 1,4-butanediol diacrylate to retain its spherical morphology and size during melt blending with a matrix material and subsequent molding of the blends. The glass-transition temperature  $T_g$  of the core material measured by a dynamic mechanical test was about  $-40^\circ\text{C}$ . Core-shell particles have a 40 wt% rubbery core. The preparation of the core-shell particles was described previously.<sup>10,11</sup> Core-shell particles were blended with PC pellets using a Brabender internal mixer (Duisburg, Germany) at  $220^\circ\text{C}$  for 10 min. The content of core-shell particles in blends was 10 wt% (rubber phase content is 4 wt%).

#### Specimen preparation, mechanical test, and microscopy

Blends were compression molded into 5-mm-thick plates at  $220^\circ\text{C}$ . The molded plates were machined into a Charpy impact bar ( $12.6 \times 5 \times 120$  mm). The Charpy impact strength was determined using a single-edge notched specimen at room temperature. The notch radius was varied from zero to 6 mm and the notch depth was 2.5 mm. The notch was produced in its desired radius by using a drill at room temperature. Fracture surfaces of the specimens were examined using a scanning electron microscope (SEM), Hitachi S-570 (Tokyo, Japan). Samples were coated with a thin layer of gold-palladium.

## RESULTS AND DISCUSSION

#### Fracture surface

It is already known that a ductile polymer such as PC fractures in a brittle manner when it contains a deep notch and plane stress state is maintained. Also, it has already been reported that the brittle fracture of the notched PC and rubber-toughened PC sheets occurs from the internal crazes, which are nucleated at the tip of the local plastic zone ahead of the notch tip.<sup>8,9,12,13</sup>

Scanning electron micrographs of the fracture surfaces of neat PC specimens with a different notch radius are shown in Figure 2. In the case of specimens with a sharp notch, the crack was initiated at the notch tip and fractured in a brittle manner [Fig. 2(a)]. However, as the notch radius increases, the nucleus for internal crazing was clearly observed inside the elliptical region in the micrographs [Fig. 2(b)–(d)]. The nucleus is definitely a nucleation site for internal crazing. In these cases, the local plastic zone was initiated from the notch tip and grew outward with as applied

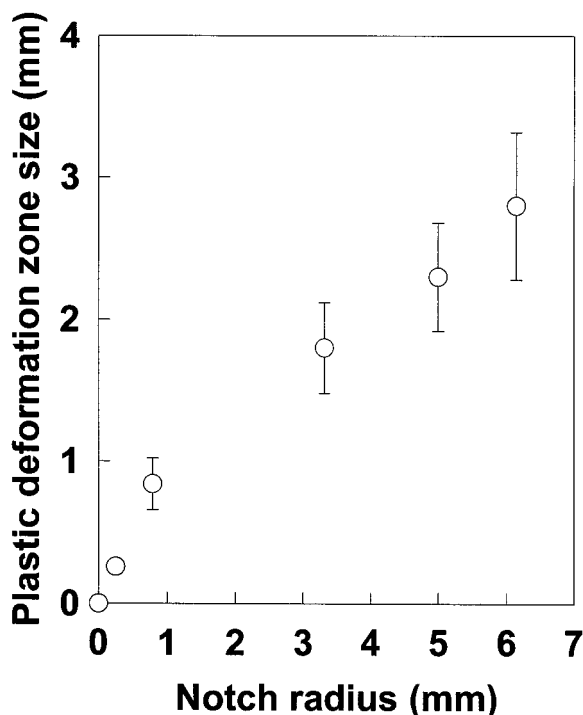
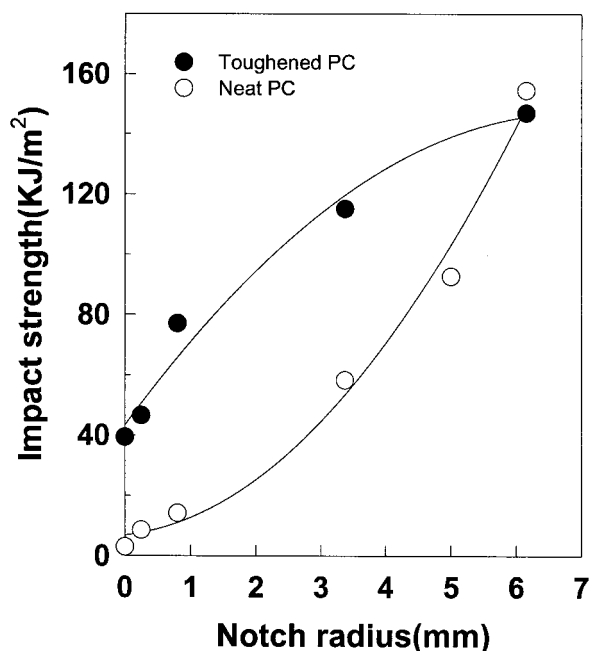


Figure 3 Plastic deformation zone size of neat PC as a function of notch radius.

stress was increased. When the mean stress reached the critical value for craze initiation, the internal craze was nucleated at the tip of the plastic zone and propagated immediately throughout the specimen, which resulted in a fracture of the specimen in a brittle manner. Thus, the distance from the notch tip to the nucleation site of the internal craze is directly related to the size of the plastic deformation zone  $r_p$ .

#### Notch sensitivity of neat PC

The plastic deformation zone size  $r_p$  of the PC specimen, containing various notch radii, is plotted in Figure 3 as a function of the notch radius. The plastic deformation zone size was determined by examining the fracture surface using an optical microscope. As can be seen in Figure 3, the plastic deformation zone size shows a linear relationship with the notch radius for a relatively small notch radius (up to 0.79 mm) as predicted by eq. (7). However, as the notch radius increases, the relationship deviates from linearity. This deviation is due to the reduction of the lateral dimension of the specimen during deformation. During the impact test, the specimen is elongated in the vertical direction, which results in reduction of the lateral dimension. The reduction of the lateral dimension varies with the notch radius. In the case of a relatively sharp notch, the reduction in the lateral dimension is small because a high level of triaxial stress is developed around the notch tip. However, as the notch



**Figure 4** Impact strength of neat PC and toughened PC as a function of notch radius.

radius increases, severe elongation occurs along the vertical direction during an impact test, similar to a necking in the tensile test. Thus, the reduction in the lateral dimension becomes larger for a more blunt notched specimen, which results in a deviation of the linearity in the plot of the plastic deformation zone size versus the notch radius (Fig. 3).

The impact strengths of neat PC and rubber-toughened PC are shown as a function of the notch tip radius in Figure 4. Also, the data regarding the impact strength in Figure 4 are replotted in Figure 5 as a function of the square of the notch radius. As can be clearly seen in Figure 5, the impact strength of neat PC shows a good linear relationship with the square of the notch radius. Therefore, it can be concluded that the proposed model significantly correlates the impact strength and the notch tip radius for ductile polymers. However, for rubber-toughened PC, this linear relationship no longer holds. The reason for the breakdown of the linear relationship will be discussed further in a section following the examination of the fracture surfaces of toughened PC.

#### Effect of incorporation of rubber particles

The fracture surface of toughened PC with a 0.25-mm notch radius is shown in Figure 6. The specimen contains 10 wt% of core-shell rubber particles. The net rubber content is only 4 wt% and the rubbery core size is 0.32  $\mu\text{m}$ . Nucleation sites of internal crazes, which can be easily seen on the fracture surfaces of neat PC, cannot be observed. The same results were obtained

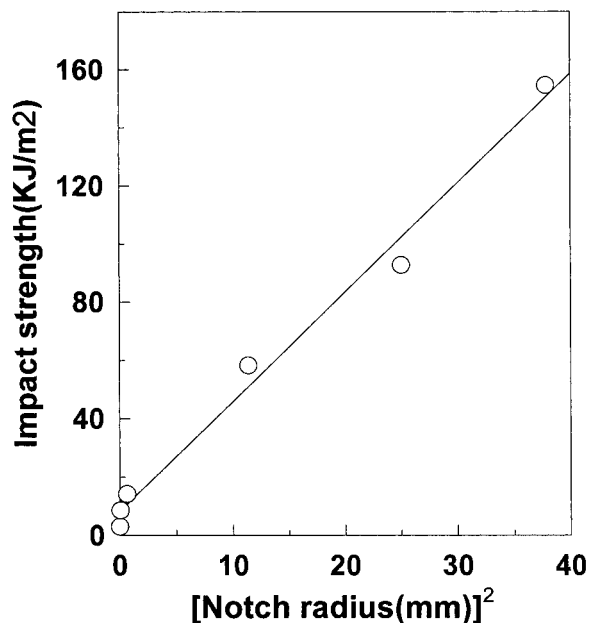


**Figure 5** Impact strength of neat PC as a function of the square of the notch radius.

for other toughened PC specimens with different notch radii, that is, the nucleation sites for internal crazes cannot be observed (Fig. 7).

It is worthwhile to compare the impact fracture behavior of PC and rubber-toughened PC. In the case of PC, for a sharp notched specimen the fracture was initiated at the notch tip and propagated throughout the specimen. For a blunt notched specimen, large-scale shear deformation occurred before the initiation of internal crazes. At critical stress, crazes were initi-

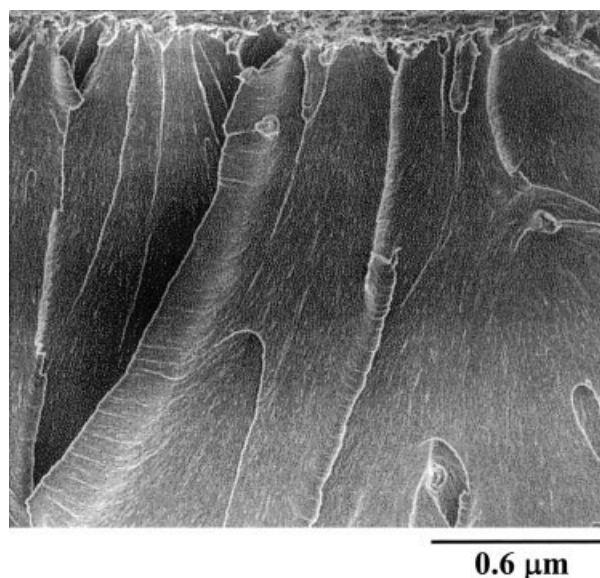


**Figure 6** SEM micrographs of the fracture surface of toughened PC. Rubber phase content: 4 wt%; notch radius: 0.25 mm. Crack propagation direction:  $\rightarrow$

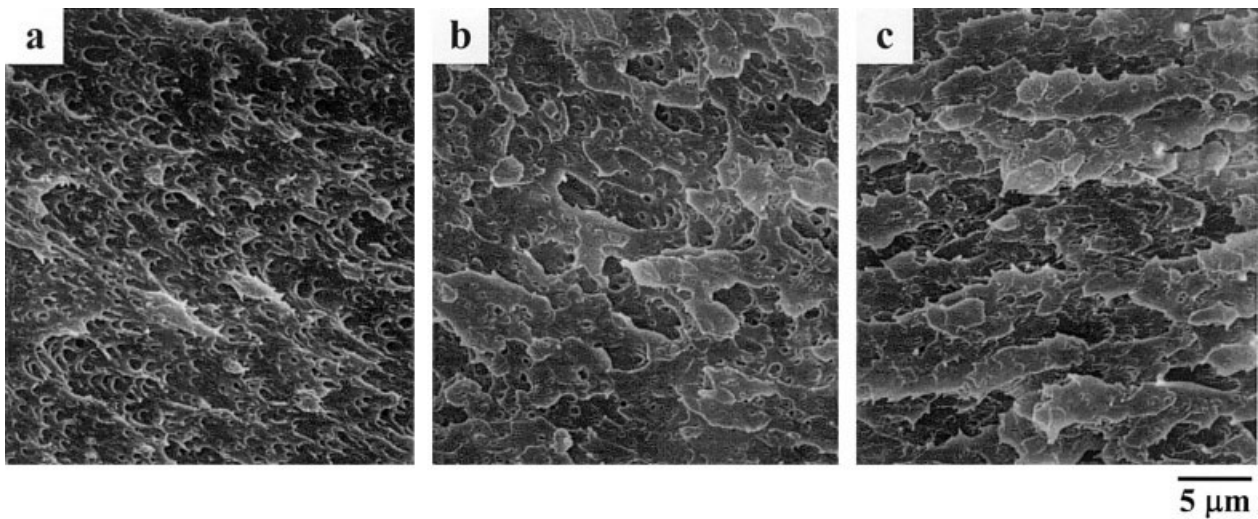


**Figure 7** SEM micrographs of the fracture surface of the crack tip region of rubber-toughened PC with a different notch radius. Notch radius: (a) sharp notch, (b) 0.25 mm, and (c) 6.15 mm.

ated at some distance away from the notch tip. Thus, in that case, most of the energy was dissipated during the shear deformation process before catastrophic fracture occurred by crazing.

In the case of rubber-toughened PC, the role of rubber particles in the failure process needs to be considered. When the mean stress reaches a critical value for internal cavitation of rubber particles or interfacial failure at the particle–matrix interface, rubber particles are cavitated, or else interfacial failure occurs at the interfaces. In this case, three different regions coexist near the notch tip, namely, the plastic region without cavity, the plastic region with cavity, and the elastic region existing continuously from the notch tip. This situation is schematically shown in Figure 8. When the void is formed in the specimen, triaxial stress is released, which results in decreases in mean stress.<sup>9</sup> Therefore, the mean stress does not reach to the critical level for initiation of craze. Thus, the internal crazing cannot occur for the toughened PC. Rubber particles play a roll in preventing the

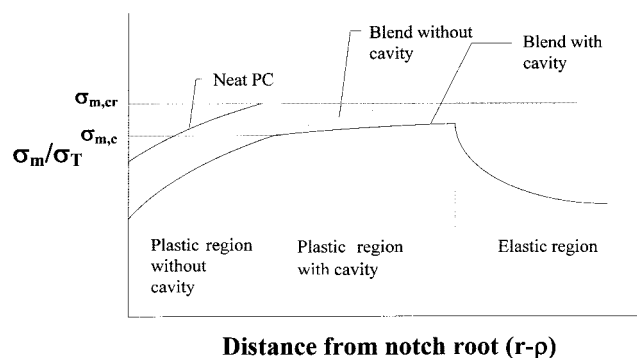


**Figure 8** Schematic diagrams illustrating the deformation zone of toughened PC.

initiation of craze inside the plastic region by decreasing mean stress through the cavitation of rubber particles or interfacial failure at the interfaces in macroscale, as well as inducing matrix shear deformation as a stress concentrator.

Toughened PC is fractured by shear deformation, whereas the fracture of neat PC is initiated by internal crazing after shear deformation, as discussed in the previous section. Since craze fracture is a very brittle process as compared to shear deformation, the fracture energy of neat PC is mainly absorbed by shear deformation. Therefore, the toughening effect by rubber particles is enhanced by suppressing the crazing

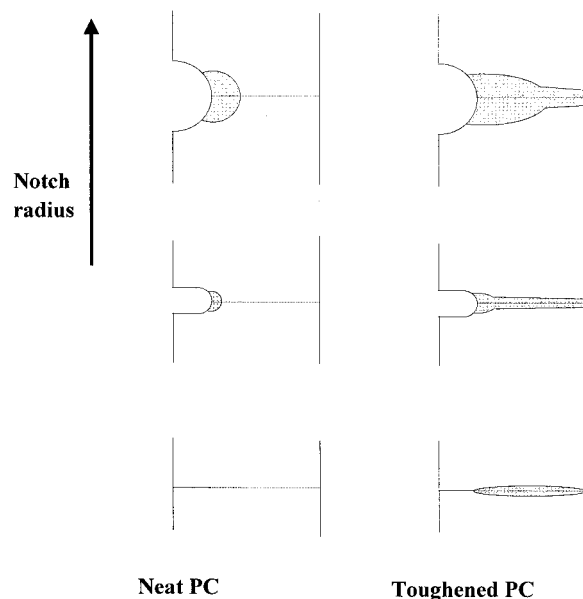


**Figure 9** Schematic diagrams illustrating the size of the deformation zone of neat PC and toughened PC.

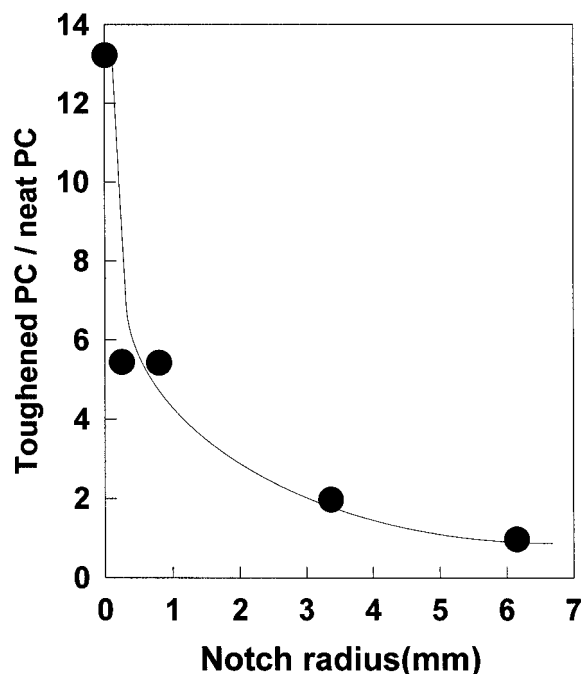


Figure 10 Ratio of impact strength of toughened PC and neat PC as a function of notch radius.

process and inducing shear deformation. The size of the shear deformation zone is directly proportional to energy absorption and is quite different for neat PC and rubber-toughened PC, even those with the same size of notch radius. The relative size of the shear deformation zone for neat PC and rubber-toughened PC with a different notch radius is drawn schematically in Figure 9. The size of the shear deformation zone of neat PC is decreased as the notch radius is decreased (see Fig. 9). On the other hand, in the case of toughened PC, the decrease of the shear deformation zone with a decrease of the notch radius is not as large compared to the neat PC, because the failure occurs mainly by shear deformation. Since the portion of the craze fracture energy in the total fracture energy becomes larger as the notch tip radius is decreased, the toughening effect (the relative ratio of the deformation zone size for toughened PC and neat PC), becomes larger as the notch tip radius becomes smaller, as shown in Figure 9. The ratio of the impact strength of toughened PC to neat PC is shown in Figure 10. The impact strength of toughened PC with a sharp notch is larger than that of neat PC by a factor of about 15. This ratio is decreased dramatically as the notch tip radius is increased.

As previously shown in Figure 4, the impact strength of rubber-toughened PC is not proportional to the square of the notch radius, as in the case of neat PC. This is due to the fact that the suggested model is based on the assumption that the fracture is initiated by internal crazing. However, for rubber-toughened PC, internal crazing does not occur because the mean stress is lowered, as shown in Figure 6, due to the cavitation of rubber particles or interfacial failure at the particle–matrix interface. That is the reason why the impact strength of toughened PC is not proportional to the square of the notch radius.

## CONCLUSION

A simple model based on the slip-lines field theory was proposed to rationalize the notch tip sensitivity of ductile polymers. The impact strength of neat PC was proportional to the square of the notch tip radius, which is in good agreement with that predicted by the proposed model. This model can be applied to material similar to PC with very large plastic deformation around the notch tip. The increase of the impact strength for toughened PC with increased notch radius is not as large as that of neat PC, which implies that inclusion of rubber particles reduces the notch sensitivity for rubber-toughened PC.

Support of this work by the National Research Laboratory Program (Ministry of Science and Technology of Korea) and BK 21 Program (Ministry of Education and Human Resources Development of Korea) is gratefully acknowledged.

## References

1. Kinloch, A. J.; Willams, J. G. *J Mater Sci* 1980, 15, 1823.
2. Vincent, P. I. *Impact Test and Service Performance of Thermoplastics*; Plastics Institute: London, 1971.
3. Fraser, R. A.; Ward, I. M. *J Mater Sci* 1974, 19, 1624.
4. Fraser, R. A.; Ward, I. M. *J Mater Sci* 1977, 12, 459.
5. Kinloch, A. J.; Young, R. J. *Fracture Behavior of Polymers*; Applied Science: London, 1983.
6. Hill, R. *The Mathematical Theory of Plasticity*; Oxford University Press: Oxford, 1950.
7. Kachanov, L. M. *Foundations of the Theory of Plasticity*; North-Holland: Amsterdam, 1971.
8. Ishikawa, M.; Narisawa, I.; Ogawa, H. *J Polym Sci Polym Phys Ed* 1977, 15, 1791.
9. Ishikawa, M.; Chiba, I. *Polymer* 1990, 31, 1232.
10. Cho, K.; Yang, J. H.; Park, C. E. *Polymer* 1997, 38, 5161.
11. Cho, K.; Yang, J. H.; Park, C. E. *Polymer* 1998, 39, 3073.
12. Parker, D.S.; Sue, H-J.; Huang, J.; Yee, A. F. *Polymer* 1990, 31, 2276.
13. Cheng, C.; Hiltner, A.; Baer, E.; Soshey, P. R.; Mylonakis, S.G. *J Appl Polym Sci* 1995, 55, 1691.